Geochemistry Geophysics Geosystems G3
AN ELECTRONIC JOURNAL OF THE EARTH SCIENCES
Published by AGU and the Geochemical Society

Article
Volume 11, Number 2
12 February 2010
Q0AB04, doi:10.1029/2009GC002715
ISSN: 1525-2027

Birth of a volcanic margin off Argentina, South Atlantic

Dieter Franke, Stefan Ladage, Michael Schnabel, Bernd Schreckenberger, Christian Reichert, and Karl Hinz
Bundesanstalt für Geowissenschaften und Rohstoffe, Stilleweg 2, D-30655 Hannover, Germany (dieter.franke@bgr.de)

Marcelo Paterlini, Juan de Abelleyra, and Miguel Siciliano
Servicio de Hidrografía Naval, Av. Montes de Oca 2124, C1270ABV Buenos Aires, Argentina

[1] Based on a dense grid of multichannel reflection seismic lines we study the evolution of a volcanic rifted margin segment off Argentina. The segment under study is located between 44°S and 41°S. We describe in detail the facies of the extrusive basaltic complexes across the margin. These include single and multiple Inner Seaward Dipping Reflectors (SDRs) with varying architecture along the margin, Outer Highs, and Outer SDR wedges. A detailed interpretation of a transitional zone between the Inner and Outer SDR wedges is presented. Multiple Inner SDRs are concentrated at the southern part of the margin segment, while in the north only one steeply dipping wedge is present. The dip of the Inner SDR wedges changes along the margin, and we propose subsidence by loading as main cause. The transitional zone between the Inner and Outer SDR wedges becomes narrower toward the north. By correlating with magnetic data we conclude that the emplacement of the 30–100 km wide multiple Inner SDRs occurred episodically. We propose an injection center which migrated in a seaward direction with proceeding extension as the origin for the multiple Inner SDRs. A scissor-like opening of the margin segment resulted in different amounts of stretching along-strike of the margin segment and is likely the cause for the varying distribution of the extrusive basaltic complexes. The varying extension rates within the margin segment contribute to decreasing volumes of melts generated in a northward direction within this rift segment.

Components: 9834 words, 12 figures, 1 table.

Keywords: volcanic passive margin; Argentina continental margin; rifting; variability of oceanic crust; Seaward Dipping Reflectors.

Index Terms: 8109 Tectonophysics: Continental tectonics: extensional (0905); 3002 Marine Geology and Geophysics: Continental shelf and slope processes (4219); 9360 Geographic Location: South America.

Received 2 July 2009; **Revised** 1 December 2009; **Accepted** 4 December 2009; **Published** 12 February 2010.

Franke, D., S. Ladage, M. Schnabel, B. Schreckenberger, C. Reichert, K. Hinz, M. Paterlini, J. de Abelleyra, and M. Siciliano (2010), Birth of a volcanic margin off Argentina, South Atlantic, *Geochem. Geophys. Geosyst.*, *11*, Q0AB04, doi:10.1029/2009GC002715.

Theme: Magma-Rich Extensional Regimes
Guest Editors: R. Meyer, J. van Wijk, A. Breivik, and C. Tegner

1. Introduction

[2] Volcanic rifted margins are characterized by thick wedges of volcanic flows [*Eldholm et al.*, 1995; *Hinz*, 1981; *Mutter et al.*, 1982; *White et al.*, 1987] and form the majority of passive margins worldwide [*Menzies et al.*, 2002; *Skogseid*, 2001]. It is generally agreed that the southern South Atlantic margins (Figure 1; between the Walvis/Rio Grande Ridges and the Falkland–Agulhas Fracture Zone) are of the volcanic rifted margin type [*Bauer et al.*, 2000; *de Vera et al.*, 2010; *Franke et al.*, 2007; *Gladczenko et al.*, 1997; *Hinz et al.*, 1999; *Hirsch et al.*, 2009; *Schnabel et al.*, 2008]. Traditionally, active rifting models (driven by a thermal anomaly or a plume) were invoked as an explanation for the formation of volcanic rifted margins. However, recent research on volcanic rifted margins indicates that their evolution is more complex than that defined by earlier models and alternative models have been suggested [e.g., *Foulger and Natland*, 2003; *Menzies et al.*, 2002; *Meyer et al.*, 2007]. There is considerable controversy on the mechanism responsible for the production of large volumes of basaltic volcanism [e.g., *Menzies et al.*, 2002] and over whether plumes initiate rifting, or rifting focuses plume activity [e.g., *Ebinger and Sleep*, 1998; *Foulger and Natland*, 2003; *King and Anderson*, 1998; *White and McKenzie*, 1989]. Investigations of the large-volume basaltic complexes from different locations are crucial for testing the models on the formation of volcanic rifted margins and the mode and driving forces for continental breakup.

[3] Here we report on a study on the basaltic extrusives off the coast of Argentina based on a dense grid of 2-D multichannel reflection seismic (MCS) data (Figure 1). This study provides a detailed investigation of the volcanic/magmatic edifices across the margin and their variations along the margin segment. We concentrate on a segment between the Colorado and the Ventana transfer zones, between 41°S and 44°S; and present previously unpublished seismic lines and geophysical data. Estimates of the extent and thickness of the basaltic extrusives are presented, providing evidence for an episodic emplacement of the multiple Inner Seaward Dipping Reflectors (SDRs). Therefore, we propose a seaward migrating injection center as the origin of the multiple SDR wedges. The transitional zone between the Inner and Outer SDR wedges that becomes narrower toward the north is discussed in detail. The change from magma-poor to magma-rich rifting takes place within about 10 km. This abrupt change leads us to consider an alternative scenario rather than solely gradual variations in the thermal structure of the mantle during breakup.

[4] We propose a scissor-like opening of the studied margin segment, which explains the migrating injection center of the multiple SDR wedges in the south and the stacked SDRs in the north. In this context, we discuss how the varying extension rates within the margin segment contribute to varying volumes of melts generated along strike of the margin.

2. Geological Framework

[5] The Early Cretaceous opening of the South Atlantic occurred diachronously, progressing from South to North [e.g., *Austin and Uchupi*, 1982; *Martin*, 1987; *Rabinowitz and Labrecque*, 1979; *Sibuet et al.*, 1984; *Uchupi*, 1989]. The rift propagated from the south toward the Tristan da Cunha hot spot [*Martin*, 1987]. The early stage of the rifting and opening of the South Atlantic (150–84 Ma) may be described as a successive northward unzipping of rift zones [e.g., *Jackson et al.*, 2000; *Nürnberg and Müller*, 1991].

[6] Rift progression seems to be controlled not only by plate kinematics, but also by the inherited lithospheric structure [*van Wijk and Blackman*, 2005]. Transfer zones are considered to be zones that delay the rift to drift transition [e.g., *Courtillot*, 1982; *Dunbar and Sawyer*, 1989]. Such zones could be formed, for example, by variations in rheological properties of the crust, an abnormally thickened crust or a less favorably oriented weak trend, stemming from earlier tectonic events [*van Wijk and Blackman*, 2005]. In addition to the major fracture zones in the South Atlantic, like the Falkland-Agulhas and the Equatorial Fracture Zone [*Uchupi*, 1989], *Franke et al.* [2007] identified four major transfer zones at the volcanic Argentine/Uruguayan margin in the South Atlantic (Figures 1 and 2). These are the Falkland Fracture Zone/Falkland transfer zone, the Colorado transfer zone, the Ventana transfer zone and the Salado transfer zone (Figure 1). These four interpreted transfer zones were recently confirmed on the basis of magnetic and gravimetric data [*Blaich et al.*, 2009]. Huge transverse structural lineaments were also found onshore South America [*Jacques*, 2003a, 2003b]. In location and trend these lineaments match the offshore transfer zones and may be their onshore continuations. This is consistent

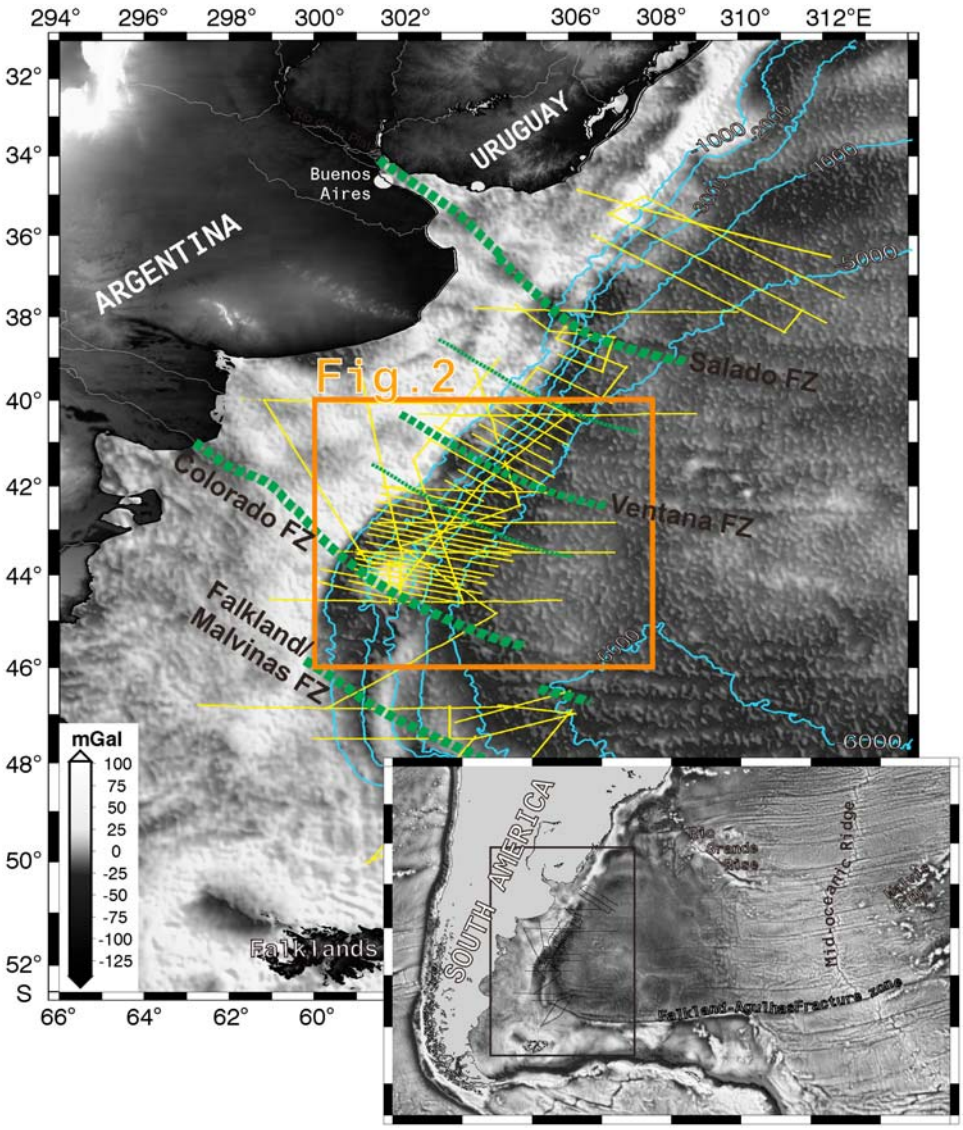

Figure 1. Study area in the western South Atlantic and location of multichannel seismic reflection lines (yellow lines). Satellite-derived gravity field [*Sandwell and Smith*, 1997] is shown for the offshore area. Transfer zones [*Franke et al.*, 2007] are indicated as dashed green lines. The inlay shows an overview map of the western South Atlantic and the study area between the Falkland-Agulhas Fracture Zone and the Rio Grande Rise/Walvis Ridge.

with studies that propose some degree of deformation of the South American plate along intraplate boundaries that were active before and during the breakup of the South Atlantic [*Eagles*, 2007; *Nürnberg and Müller*, 1991; *Unternehr et al.*, 1988].

[7] Continental breakup and initial seafloor spreading in the South Atlantic were accompanied by extensive transient volcanism and magmatism as inferred from sill intrusions, flood basalt sequences, voluminous volcanic wedges, and high-velocity lower crustal bodies. In seismic reflection data the voluminous extrusives are manifested by huge wedges of Seaward Dipping Reflectors (SDRs) on both sides of the southern South Atlantic [*Franke et al.*, 2007; *Gladczenko et al.*, 1997, 1998; *Hinz et al.*, 1999]. Industry drilling off Namibia (Kudu Field) show that lavas were erupted subaerially [*Clemson et al.*, 1999]. *Schnabel et al.* [2008] reported that high-velocity lower crustal bodies are present beneath the Argentine margin and interpreted these as underplated material. SDRs are usually considered as part of large igneous provinces, formed during highly episodic and short-lived (<1 ± 3 Ma) pulses of large-volume magmatism [*White and McKenzie*, 1989]. Direct sampling by drilling of SDRs on the Rockall and

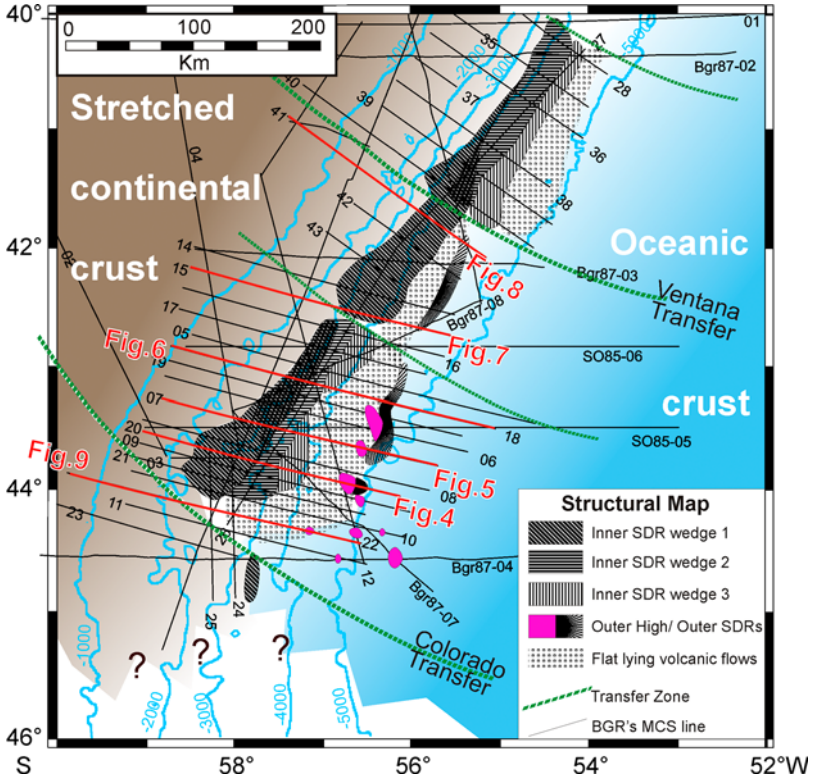

Figure 2. Structural map showing the distribution of extensive volcanics manifested by thick wedges of Seaward Dipping Reflectors (SDRs) and additional volcanic/magmatic features. Transfer zones and margin segmentation as interpreted from *Franke et al.* [2007]. Blue lines show the water depth every 1000 m. Line numbers without a prefix were acquired during the BGR98 survey. Locations of example seismic sections shown in Figures 4–9 are indicated. For location see Figure 1.

Norwegian margins confirmed that they are composed of basaltic rocks [e.g., *Leg 104 Shipboard Scientific Party*, 1986; *Roberts et al.*, 1984a, 1984b] and the East Greenland drilling proved that the basalts were emplaced subaerially [*Larsen and Saunders*, 1998].

3. Data and Processing

[8] In this study we concentrate on one segment of the southwest Atlantic margin located between 44°S and 41°S that is particularly well covered by seismic lines (Figure 2). Between 1987 and 2004, the Federal Institute for Geosciences and Natural Resources (BGR) conducted an extensive program of deep seismic reflection profiling off the coast of Argentina and Uruguay (Figure 1). The geophysical data described in this paper were acquired predominantly during the BGR98 survey using the seismic vessel Akademik Lazarev. Differential Global Positioning System (DGPS) was implemented using a Trimble (MFX) GPS receiver as a primary and a GPS Sercel NR-103 receiver as a secondary unit interfaced to the RGP-2D system and Skyfix for the differential corrections. The GPS system provided 24 h coverage per day with an average of seven satellites in sight. The positioning using DGPS throughout the survey resulted in an absolute accuracy that was better than 10 m.

[9] The energy for the seismic reflection study was generated by an air gun array consisting of four linear subarrays with a total of 32 air guns. Each of these subarrays consisted of eight air guns, type BOLT 1900 LL-X with chamber volumes varying between 0.62 L and 3.28 L. Thus the maximum total volume used during cruise was 69.8 L. Sausage buoys were used as floating devices to maintain a towing depth of 7.5 m ± 0.5 m. Each subarray had a total length of 15 m. The working pressure was 2,000 psi (13.8 MPa). An equidistant shot interval of 50 m was used for the reflection seismic lines.

[10] For data acquisition a 4,500 m long digital SYNTRAK Type 480/16 streamer with a group length of 25 m was used. It consisted of 180

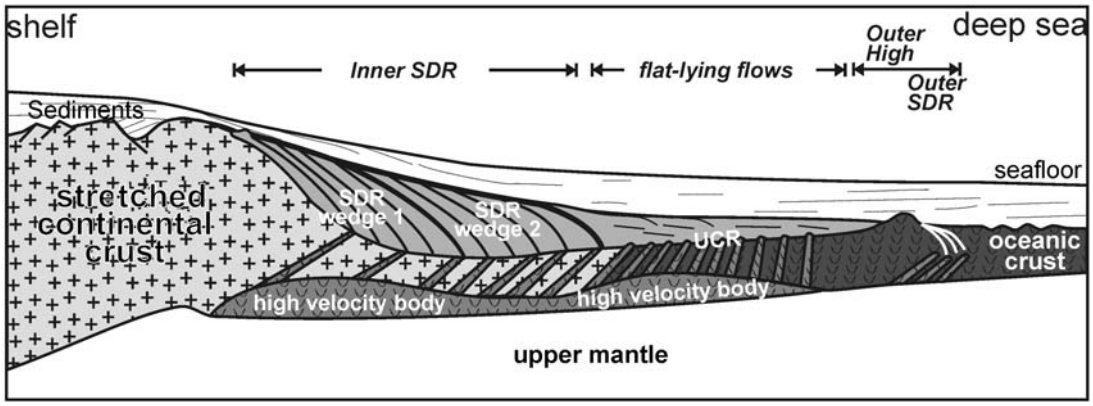

Figure 3. Sketch illustrating the main volcanic/magmatic features at the Argentine continental margin (not to scale). Beneath the slope are one or multiple Inner Seaward Dipping Reflectors (SDRs) and a high-velocity lower crustal body. Seaward prominent features are another high-velocity lower crustal body and Upper Crustal Reflections (UCR). The area farther seaward is defined by occasionally occurring Outer Highs and an SDR wedge before reaching oceanic crust.

channels with 32 type T-4 hydrophones per channel, 18 MultiTRAK depth controllers with compasses, and 17 JRC SRD-300 streamer recovery devices. The operational depth was 11 m ± 1 m. The data were recorded at a sample rate of 2 ms with a record length of 15360 ms.

[11] Processing of the MCS lines was performed up to poststack time migration. After testing various combinations of processing parameters, the following sequence was regarded as optimal. Prestack processing included resampling to 4 ms with antialias filter, geometry editing, start-of-data (SOD) correction, trace editing and muting, and true amplitude recovery. After band-pass filtering (2-4-80-120 Hz trapezoid) a predictive deconvolution was applied (operator length: 240 ms, prediction distance: 20 ms, white noise level: 1%, design window:4.5 s below seafloor for near trace, shifted 1.4 s, 3.6 s for far trace). Stacking velocities were determined at an average distance interval of 3 km. After normal moveout (NMO) correction top and bottom muting was applied plus an inner trace mute where the first ocean bottom multiple interfered with interpretable primary reflections. The stacked data (45-fold) were finally time migrated using the Stolt algorithm. Figures 4–9 and 11 show this time migrated version. We used the Schlumberger-GeoQuest software to interpret the 2-D profiles.

[12] The magnetic measurements were taken with an Elsec 7706 magnetometer system. The proton precession sensor was towed on a 200 m floating cable.

[13] Gravity was measured with a LaCoste and Romberg Model S Air-Sea gravity meter, serial number S-105. Before and after the cruise, gravity ties to land stations were done with a LaCoste and Romberg land gravity meter; model G, no. 1086 (LCR G 1086).

4. Facies of the Emplaced Volcanics and Interpretational Approach

[14] In describing the volcanic features along the Argentine margin, we mainly use the nomenclature introduced by *Planke et al.* [2000] (Figure 3). Beneath the shelf and continental slope one or multiple Inner SDR wedges covering an area of up to 100 km in an E-W direction were identified. Seaward flat-lying volcanic flows [*Franke et al.*, 2007] overlie stacks of irregular and hummocky reflections that we here refer to as Upper Crustal Reflections (UCR). Farther seaward, Outer Highs and an Outer SDR wedge are often observed. Seaward of this zone, we interpret a strong, irregular, hummocky and diffractive seismic top reflection as oceanic crust. Seismic lines extending some 100 km east of the foot of slope show that the oceanic crust is heavily dissected by normal faulting. A discontinuous reflection at the base of the oceanic crust, corresponding to the Moho indicates that the oceanic crust is about 2.0 to 2.2 s two-way time (TWT) or 5.0 to 6.0 km thick. The lower crustal structure is not fully resolved by the MCS data. However, a refraction seismic profile running perpendicular to the margin at 44°S revealed two spatially separated high-velocity bodies in the

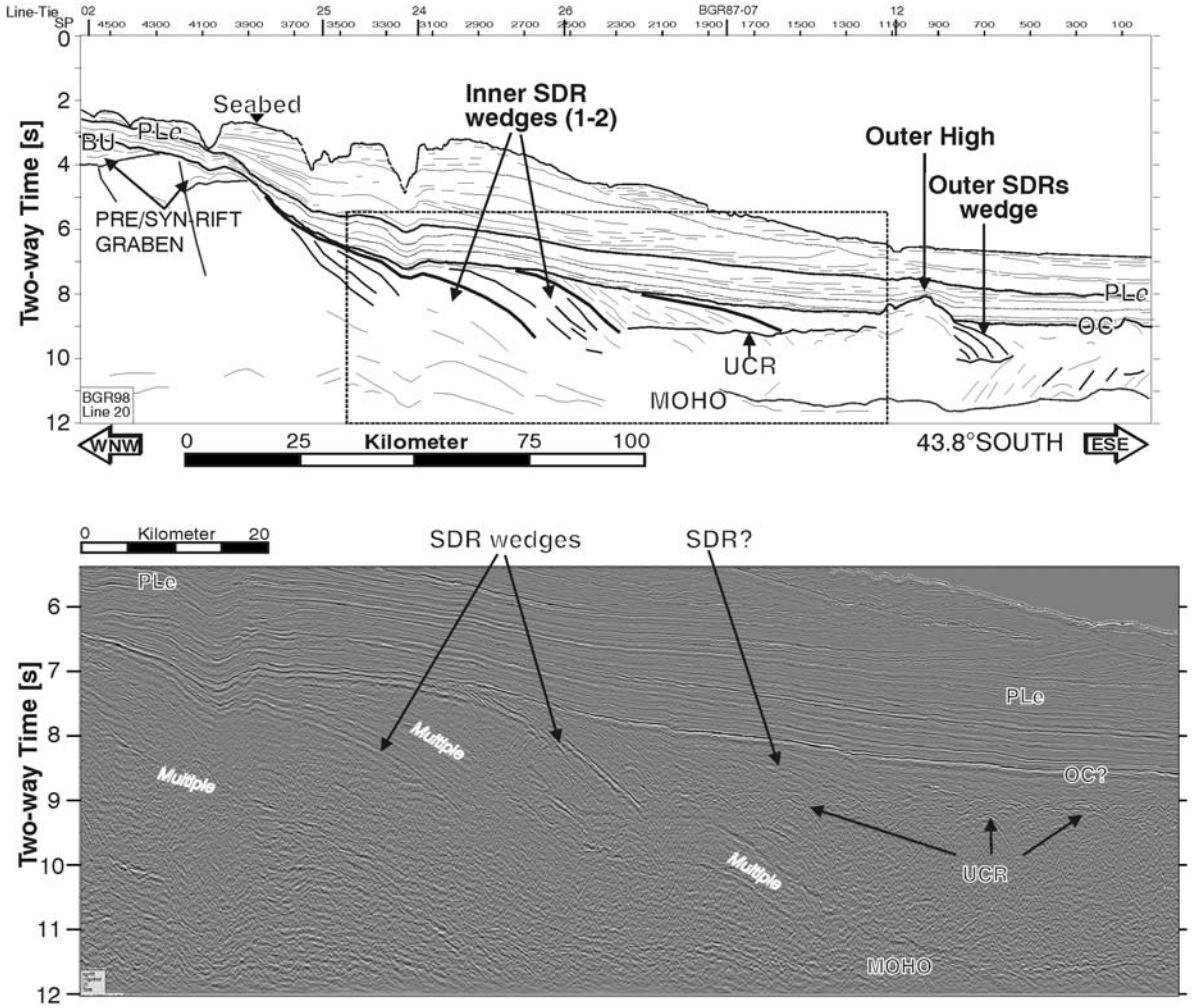

Figure 4. Seismic profile BGR98-20, located in the southern part of the volcanic margin segment under study. At least two laterally separated Inner SDR wedges developed with unconformities on top. A distinct, low-frequency horizontal reflection band at about 9 s (TWT) depth forms the Upper Crustal Reflections (UCR). On top of these reflections less distinct Seaward Dipping Reflectors (SDRs) are present. OC, top of the oceanic crust; BU, breakup unconformity; PLe, Pedro Luro Equivalent, separating Cretaceous from Tertiary postrift sediments; SDRs, Seaward Dipping Reflectors; UCR, Upper Crustal Reflections. For the location of the line see Figure 2.

lower crust [*Schnabel et al.*, 2008]. High-velocity bodies are located landward and seaward of the Inner SDRs, beneath the downsection of the Inner SDR wedges no high-velocity lower crustal body was imaged.

4.1. Inner SDRs

[15] The first manifestations of magmatism along the margin segment are prominent Inner SDR wedges (Figures 4–7). The SDRs are generally wedge shaped and convex upward. The magnetic data suggests that parts of the steeply dipping acoustic basement adjacent to the Inner SDR wedges may be overlain by thin volcanic flow units. The landward limit of the Inner SDRs in the reflection seismic data often exhibits a distinct feather edge, forming minor escarpments with an elevation of some 200–500 ms (TWT) (e.g., Figure 5). The top reflection from the landward Inner SDRs generally shows a strong, continuous, low-frequency pattern. This reflection continues in a landward direction across the feather edge into the breakup unconformity [*Franke et al.*, 2006, 2007; *Hinz et al.*, 1999]. The unconformity is distinguished from the volcanic flows by reduced reflection amplitudes and a more irregular pattern. Internally, the SDRs show a divergent reflection pattern, with layers thickening downward and increasing dip. The internal SDR reflections vary in their reflection amplitude but are generally weaker and less continuous than the top reflection.

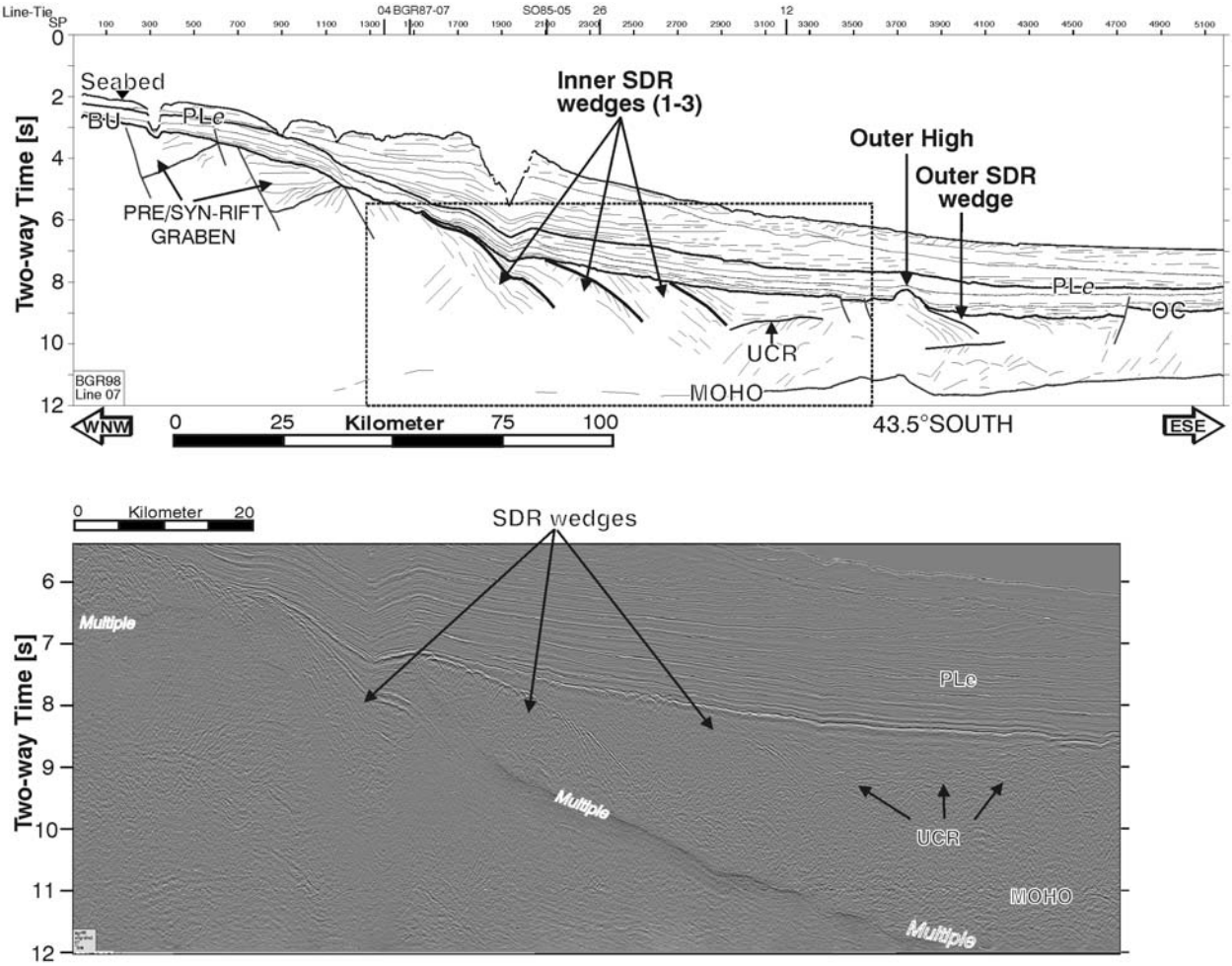

Figure 5. Seismic profile BGR98-07, located in the southern/central part of the margin segment under study. At least three inner SDRs developed laterally separated with distinct unconformities on top. The UCR are a low-frequency horizontal reflection band at about 9 s (TWT) depth. These reflections might merge with the base of the most seaward located SDR wedge. Notations are as in Figure 4; for the location see Figure 2.

There are few indications that the inner SDRs are bounded by faults.

[16] Multiple inner SDRs were mapped on the basis of following criteria: (1) the characteristic strong, continuous and smooth top reflection of a SDR unit occurs several times and delineates individual SDR bodies and (2) in map view and cross section these appear side by side and overlap only partially (Figures 4 and 5). In addition, inner SDRs dip considerably shallower where multiple SDRs are present compared to a single SDR domain. Correlation of the individual SDR units between the lines was accomplished on the basis of their seismic facies with additional constraints from the magnetic data. Two strike lines with line ties to the dip sections provided additional information on the along-margin distribution of the SDRs. It should be mentioned that we have no constraint on the absolute ages and relative timing of the SDR emplacement. It might well be that the SDR wedges were emplaced time transgressive along the margin.

[17] As a crude estimate of the volume of the emplaced volcanics we calculated the cross-sectional area of the emplaced SDR units (Table 1). Where multiple wedges partly overlay the landward wedge was given priority. We used the apparent cross-sectional area and did not project the lines onto true dip sections. Thus in the north where the seismic lines run slightly oblique to the margin, a moderate overestimate of cross-sectional area may occur. Regarding the overall uncertainty this error is negligible. To derive the vertical thickness of the SDR units we geometrically flattened the seismic section along the SDR top reflection and then picked the maximum depths of the arcuate reflec-

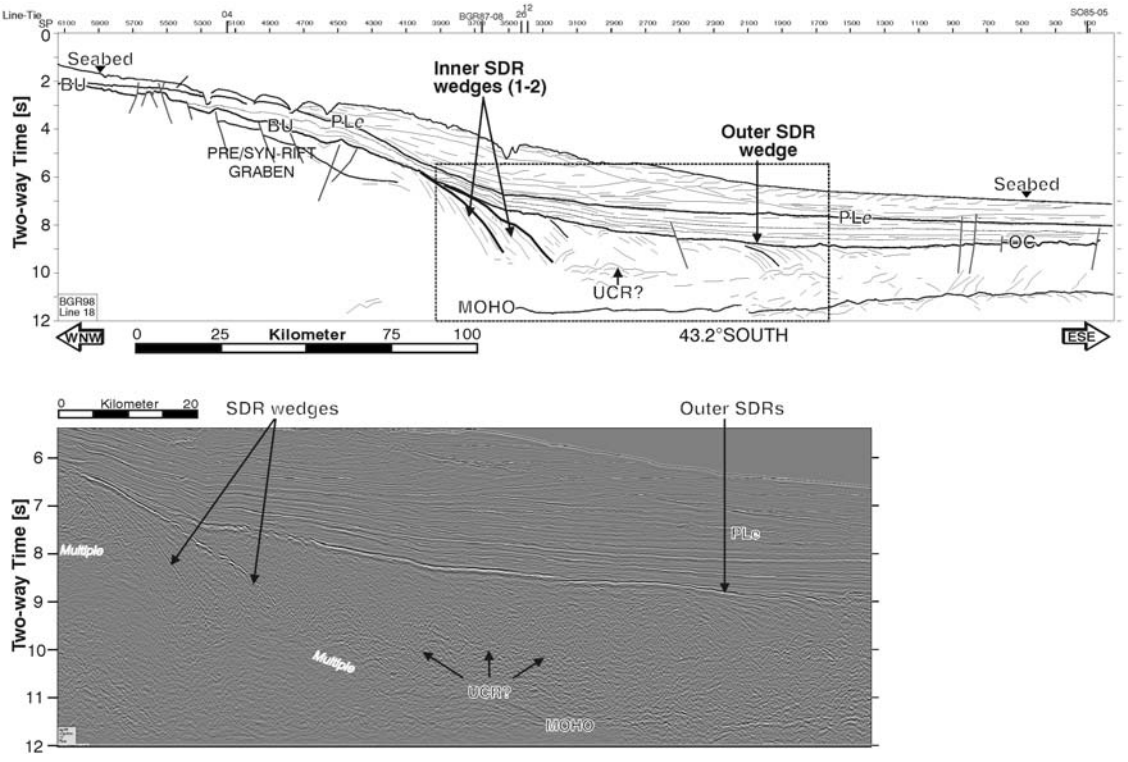

Figure 6. Seismic profile BGR98-18, located in the central part of the margin segment under study. Inner SDR wedge 1 becomes increasingly buried beneath wedge 2. The UCR are interpreted at about 10 s (TWT) depth and might merge with the base of the most seaward located SDR wedge. This reflection represents the base of the seaward Outer SDRs. Notations are as in Figure 4; for the location see Figure 2.

tions. The estimation of the maximum vertical thickness in seconds (TWT) has considerable uncertainties because base reflections of the SDR units are rare. In addition, seabed multiples sometimes mask these reflections and in such cases the values given in Table 1 are minimum numbers. The thickness of the SDRs in kilometers was calculated with an average velocity of 5.8 km/s as derived from a refraction seismic study [*Schnabel et al.*, 2008]. We calculated the cross-sectional area occupied by the SDRs by assuming a triangle shape of these units. Considering all uncertainties and approximations we estimate the error in the cross-sectional areas shown in Table 1 to be as large as 25%.

4.2. Flat-Lying Flows

[18] Between the Inner and Outer SDRs there is an up to 70 km wide zone with reflection characteristics that differ from oceanic crust. This zone was described as flat-lying flows by *Franke et al.* [2007] off Argentina and by *Bauer et al.* [2000] on the conjugate margin off Namibia. However, this general term may not be meaningful enough to describe this zone. A striking feature in this zone is the presence of subhorizontal Upper Crustal Reflections (UCR) ~500 to 2000 ms (TWT) beneath the acoustic basement reflection. The acoustic basement is a prominent reflection, exhibiting strong, long-wavelength, low-amplitude undulations. The UCR are characterized by stacks of irregular and hummocky reflections about 5 km wide. The subhorizontal reflections mimic neither the basement topography, the thickness of the overlying postrift sediments, nor any intrasedimentary reflections. UCR are observed throughout the southern study area (Figures 4 and 5). In the west, the reflection band interacts/merges with the down-dip section of the most seaward located SDR wedge (Figure 5). The further seaward continuation of the UCR is ambiguous. The reflection band might merge with the interpreted top oceanic crust reflection or form the base of Outer SDR wedges. In cases where an Outer High is present we tentatively interpret that the UCR gradually merge with the top reflection of that high.

[19] The low-frequency acoustic basement reflection above the UCR passes continuously from the top oceanic crust reflection into the top SDR. Its top shows a reflection pattern that is characteristic

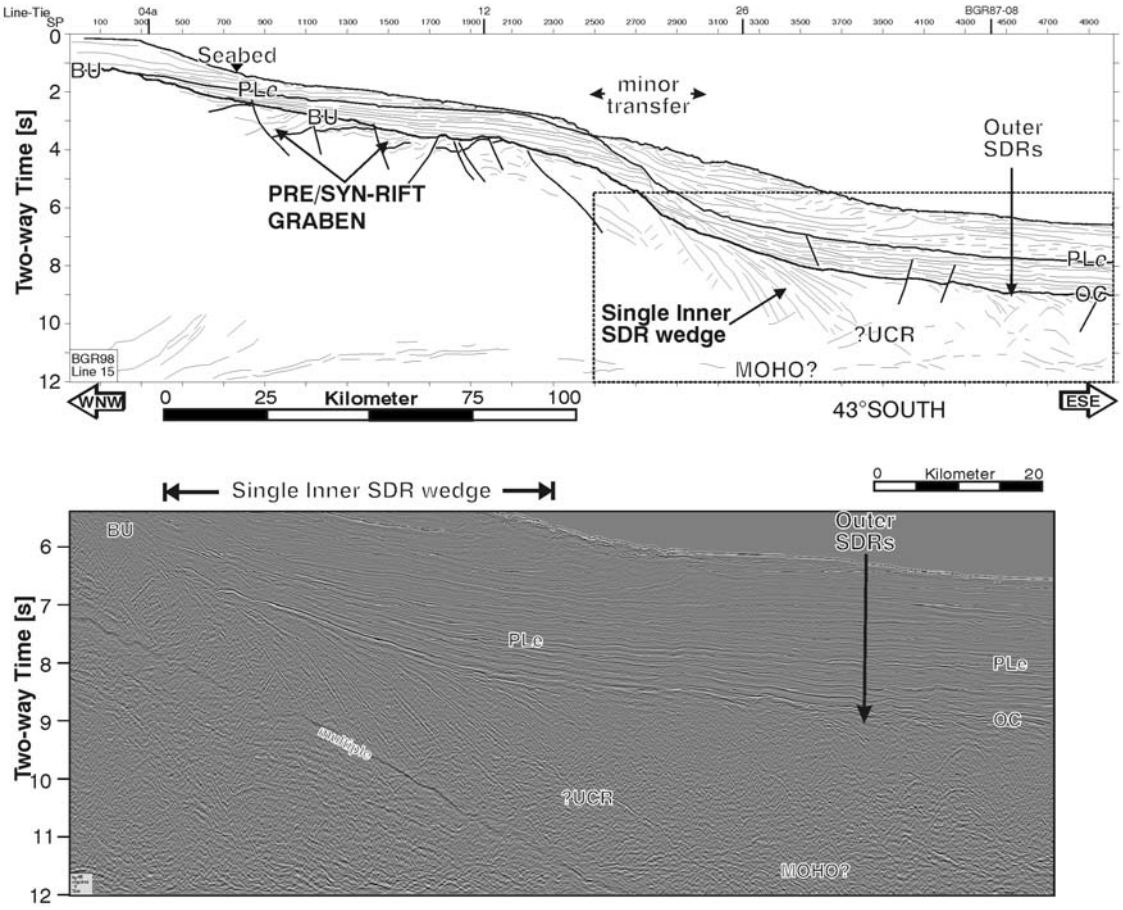

Figure 7. Seismic profile BGR98-15, located in the northern part of the margin segment under study. One single Inner SDR wedge developed that exhibits no distinct unconformity on top. The SDRs show a high-frequency arcuate internal reflection pattern. UCR are not distinct; however, a few crustal horizontal reflection elements at about 10 s (TWT) might represent this structural element. Notations are as in Figure 4; for the location see Figure 2.

of volcanics and is tentatively interpreted as such. Internally, the unit between the acoustic basement and the UCR shows much less reflections than the SDRs. If present these internal reflections exclusively dip seaward. Velocities derived from seismic refraction studies show that it is impossible to distinguish the area on top of the UCR from the SDRs or the oceanic crust [*Schnabel et al.*, 2008]. The crust between the Inner and Outer SDRs is considerably thicker than average oceanic crust and corresponds with the seaward high-velocity lower crustal body. A Moho reflection about 1–2.5 s (TWT) beneath the UCR is commonly observed.

4.3. Outer High and Outer SDR

[20] Outer Highs are steep sided, seismically chaotic, cone shaped features that are interpreted to be volcanic cones. These features occur only occasionally. Outer SDR wedges in contrast are widespread. They are typically about 25 km wide and about 1 s (TWT) thick (Figures 4 and 5). The Outer SDRs show a divergent reflection pattern with downsection thickening and increasing dip. In contrast to the inner wedges there is evidence that the Outer SDR wedges terminate against a subparallel reflection band (e.g., Figure 6) located in the midcrust. The seismic facies of this reflection band is similar to that of the UCR described above. In the oceanic domain the crust is often seismically transparent.

5. Results

5.1. Distribution of the Volcanics Along the Margin

[21] Within the margin segment SDRs are continuously present along strike (Figure 2). However, as Table 1 shows, the SDRs vary significantly in extent, thickness and volume. Although large uncertainties exist in the volume calculation, a

Table 1. Extent of the Inner SDRs Across the Margin[a]

Line in Survey BGR98	Latitude of Center SDR (°S) (Aligned Along Line 26)	Extent of SDRs Across the Margin (km)			Maximum Thickness TWT (s)	Maximum Thickness (km) (at V = 5.8 km/s)	Cross-Sectional Area (km^2) (Assuming a Right-Angle Triangle Shape)
		SDR Wedge 1	+SDR Wedge 2	+SDR Wedge 3			
41	41.74			33	2.4	7.0	115
42	41.93			40	2.0	5.8	116
43	42.21			?34+x	2.1	6.1	?104+x
14	42.39			53	2.3	6.7	177
15	42.55			47	2.4	7.0	164
16	42.71	15	32	44	2.4	7.0	153
17	42.87	19	35	58	2.4	7.0	202
05	43.03	21	37	58	2.6	7.5	219
18	43.15	26	37	46	2.6	7.5	173
19	43.25	29	41	47	2.2	6.4	150
06	43.36	34	48	56	2.1	6.1	171
07	43.53	38	57	72	2.0	5.8	209
08	43.70	57	79	98	2.0	5.8	284
20	43.80	57	79	100	2.0	5.8	290
09	43.88	56	78	93	1.8	5.2	243
21	43.99	57	80	88	1.8	5.2	230

[a] Line locations are indicated in Figure 2. The position is given for the intersection of the dip lines with the margin-parallel line BGR98-26. Line BGR98-43 did not reach the seaward end of the SDRs. The top of Table 1 is north, and the bottom is south.

considerable northward decrease of the volume of effusives is obvious (Figure 2 and Table 1).

[22] Multiple Inner SDR wedges are distinct in the southern part of the segment (Figures 4–6). Across the margin, the individual SDR units overlap only partially and are bounded by strong, continuous, and smooth top reflections that we interpret as unconformities (Figures 4 and 5). In the south the Inner SDR domain is up to 100 km wide in east-west direction. The vertical thickness increases from 1.8 s (TWT) to a maximum value of 2.6 s (TWT) where multiple wedges show a maximum overlap (Figure 6), at the northern limit of the multiple SDRs occurrence. Further north, one broad, 30 to 53 km wide SDR wedge is present with an arcuate, high-frequency internal pattern (Figures 7 and 8). Here, the SDR wedge can be traced down to almost Moho depth where it is not masked by multiples and appears to terminate against horizontal reflections (UCR?), about 1 s (TWT) above the Moho (Figure 7). The style of those volcanics resembles that found off the coast of Norway [*Planke et al.*, 2000].

[23] The western limit of the SDRs was identified at a water depth of about 2000 m at 44°S, while it is at 3500–4000 m in the northern part of the study area at 41°S. The difference in depth is not related to the thicknesses of the sediments overlying the volcanic sequences. The depth of the feather edge in two-way traveltime is 5.0 to 5.5 s in the south while it is 6.0 to 6.5 s in the north. Internally, the SDRs show a divergent reflection pattern with downsection thickening and increasing dip. This may be related to synconstructional subsidence [*Mutter et al.*, 1982]. Normal listric faults bounding the SDRs are absent in our data, indicating that subsidence was mostly due to loading as proposed by *Talwani and Abreu* [2000]. We suggest that the stacked SDRs in the northern part of the segment resulted in a heavier loading and thus in greater subsidence in comparison to the southern part of the margin segment. This interpretation is also consistent with the observation that in the northern part of the margin segment the dip of the SDRs is generally steeper than in the south. The increasing burial of the most landward flow under the next flow unit may be a widespread phenomenon in the South Atlantic. A northward increasing burial of older wedges beneath younger wedges is also reported for the Pelotas and Walvis basins to the north of the area under study [*Talwani and Abreu*, 2000].

[24] Stacks of irregular and hummocky reflections seaward of the Inner SDRs, defining the UCR, are distinct in the southern part of the margin segment (Figures 4 and 5) but in the north these are not so clear. In the south the UCR are located at about 500 ms beneath the acoustic basement reflection. Along strike of the margin the UCR show a gradual

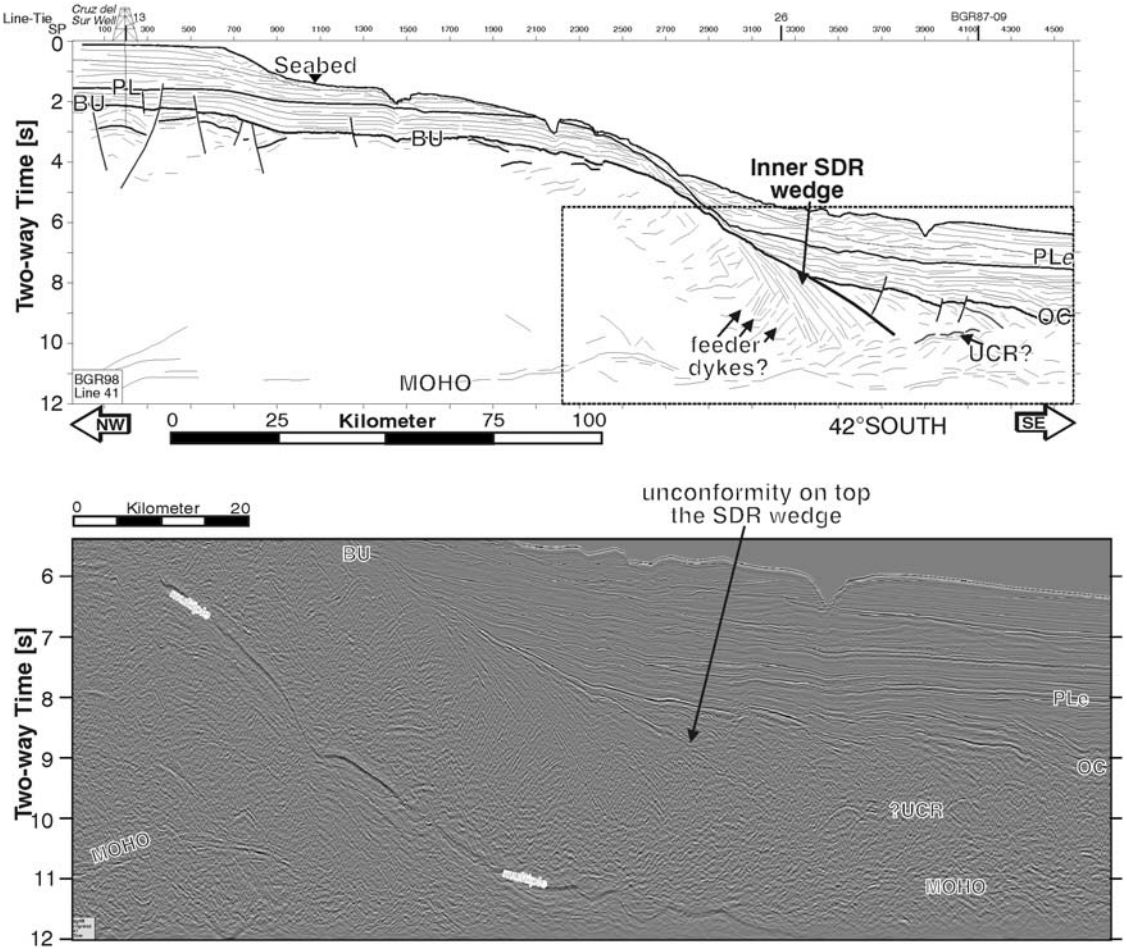

Figure 8. Seismic profile BGR98-41, located in the northern part of the margin segment under study, close to the Ventana transfer zone. One narrow, steeply dipping single Inner SDR wedge developed that exhibits an unconformity on top. Internally, the SDRs show a high-frequency arcuate reflection pattern. Landward dipping reflections beneath the SDR wedge may indicate feeder dykes. A few crustal horizontal reflection elements at about 10 s may represent the UCR. Notations are as in Figure 4; for the location see Figure 2.

increase in depth from ~0.5 s (TWT) beneath the acoustic basement at ~43.8°S (Figure 4), to 1.5 s at ~43.5°S (Figure 5), to ~2 s (TWT) at ~43°S (Figure 6), where they are only 1 s (TWT) above the Moho reflection. We suggest that the weakening of the reflections in northern direction is due to the increased burial of this reflection and that some reflection elements at about 10 s (TWT) depth along northerly lines are equivalents of the UCR (Figures 7 and 8). However, in any case it is obvious that the area between the Inner and Outer SDRs becomes increasingly narrower toward the north (see Figure 2). Although Outer Highs are sparse in the northern area, Outer SDRs are common throughout the study area. The distance between the Inner and Outer SDRs is up to 70 km in the south and it is less than 20 km in the northern part of the margin segment.

5.2. Transition to a Magma-Poor Margin Segment

[25] Figure 9 shows a profile at the transition to the margin segment between the Falklands–Malvinas Fracture Zone and the Colorado transfer zone (at ~44°S). *Franke et al.* [2007] interpreted this margin segment as a transition from a sheared to a typical volcanic margin. The WNW-ESE trending profile across the Colorado transfer zone (Figure 9) shows a steeply dipping acoustic basement, where the margin is dissected by deep normal faults. Sediment filled grabens are observed along the normal faults. The graben fill probably consists of synrift sediments including igneous volcanoclastics. Hummocky reflection bands located between the steeply dipping acoustic basement and mature oceanic crust might be an equivalent of the distinct UCR some 10 km further north. The oceanic crust

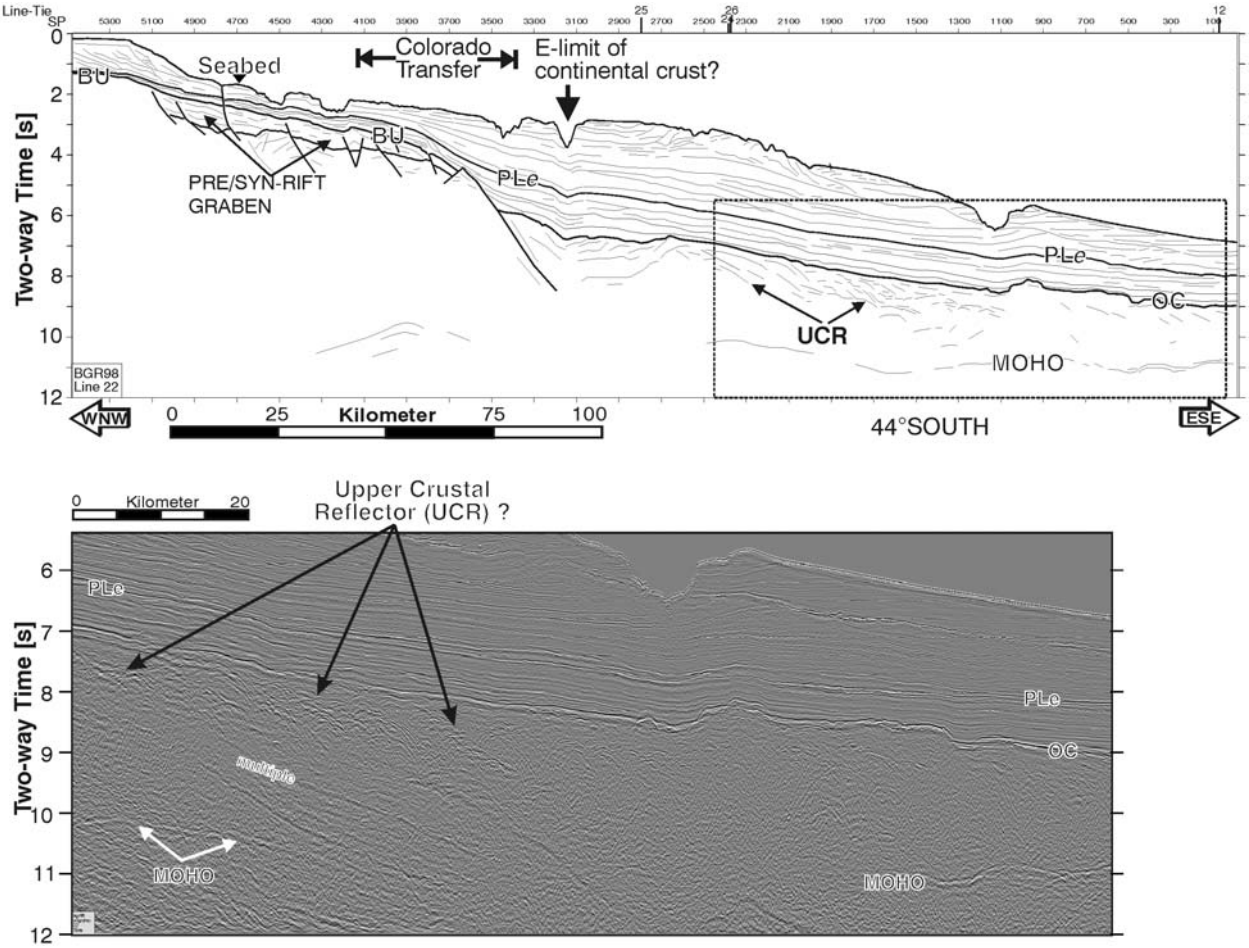

Figure 9. Seismic profile BGR98-22, crossing the Colorado transfer zone in the southern part of the margin segment under study. This line is situated in the magma-poor margin segment. The hummocky reflections beneath the basement reflection might be equivalents of the UCR further north. Notations are as in Figure 4; for the location see Figure 2.

is well imaged, with a strong top reflection that is intensively dissected by normal faults that often penetrate to Moho level. *Blaich et al.* [2009] performed gravity modeling along this line and found that the area of the graben and the hummocky reflection bands are underlain by high-density lower crustal bodies. In this gravity model, the area with reflection bands has a density equal to that of the SDRs.

5.3. Episodicity in the Emplacement of the Seaward Dipping Reflectors

[26] The fact that the multiple Inner SDR wedges off Argentina were emplaced rather side by side and overlap to a certain degree provides strong evidence for multiple phases of volcanism. This is similar to the Norwegian volcanic margin, where *Leg 104 Shipboard Scientific Party* [1986] and *Eldholm et al.* [1989] suggested overlapping successions of SDRs were emplaced by consecutive phases of volcanism. Other indicators for episodic volcanic activity off Argentina are certain characteristics of the magnetic anomalies. The magnetic signature in the area of the SDRs changes both along and across the margin (Figure 10). North of the Colorado transfer zone, in the area of the multiple SDR wedges, several magnetic anomalies and polarity reversals are observed, indicating that the individual flows were emplaced with different polarities.

[27] A distinct magnetic high over the landward SDR wedge corresponds to a normal magnetic direction while the negative anomaly over the third wedge may indicate reversed polarity of the related extrusive volcanics. The second SDR wedge corresponds to a weak magnetic high. We propose that this is caused by an interference of the magnetic signature of individual volcanic flow units. In the

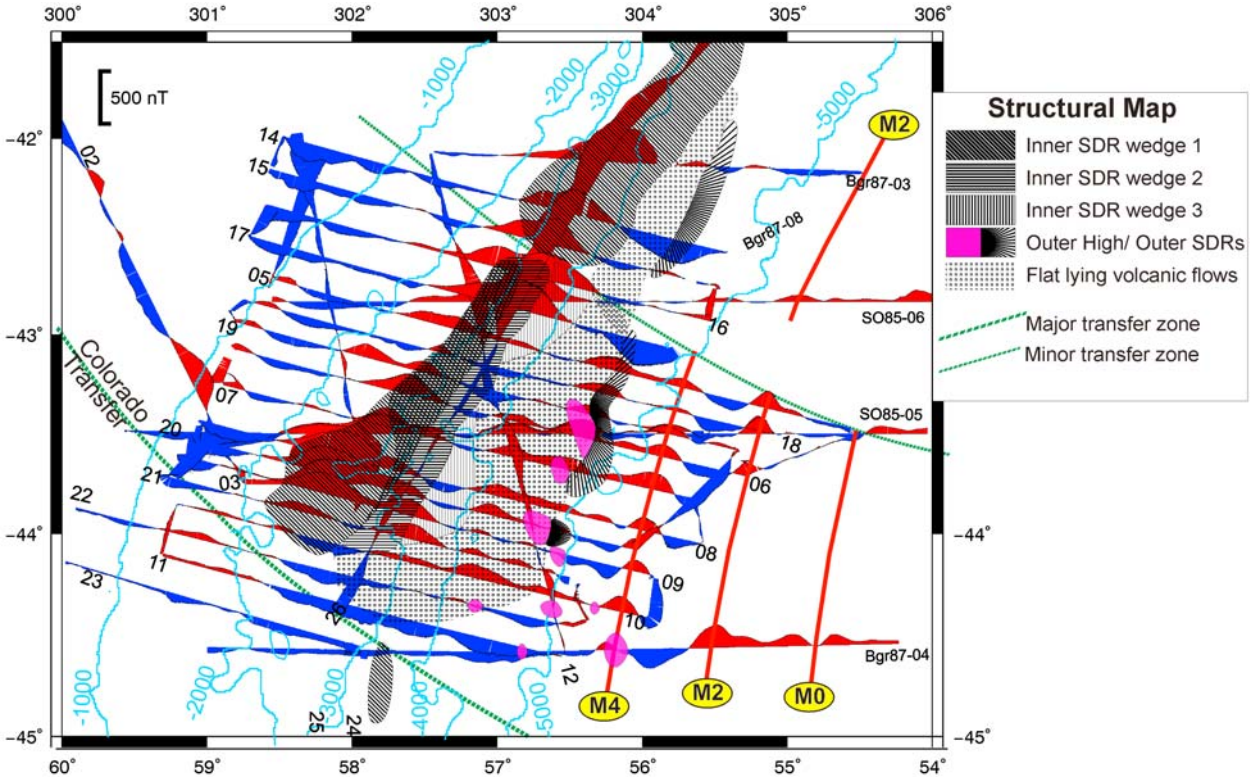

Figure 10. Structural map showing the distribution of extensive volcanics superimposed on the magnetic data recorded along the MCS lines. The individual Inner SDRs correspond to alternating magnetic highs and lows.

center of the margin segment, the amplitudes of the magnetic anomalies decrease, with the first SDR wedge corresponding to a positive and the second wedge to a negative magnetic anomaly. In the northern part of the segment, a continuous distinct positive magnetic anomaly is present at the location of the stacked SDRs (Figure 10). We propose that this magnetic high is caused by a uniform normal magnetization of the individual volcanic flows units. The Outer Highs and the Outer SDRs do not show consistent correlations with magnetic anomalies.

6. Discussion

6.1. Nature of the Upper Crustal Reflections

[28] Although there is considerable amplitude variation, we conclude from the widespread occurrence of the UCR off Argentina that this feature is an important structural zone along the margin (Figure 11). It is also present along the conjugate margin off Namibia and South Africa [e.g., *Bauer et al.*, 2000; *de Vera et al.*, 2010]. From the amplitude and frequency of the magnetic anomaly pattern, *Max et al.* [1999] interpreted this area as oceanic crust. However, the reflection characteristic of this zone is different from that of oceanic crust further seaward.

[29] We exclude the possibility of a continental origin for the UCR because these were only found seaward of where we expect continental crust to end. The SDRs are symmetrically present at both conjugate margins [e.g., *Gladczenko et al.*, 1997] and any postulated continental crust seaward of these features would cause geometrical problems when restoring the margins to the prebreakup position. In the following we discuss several scenarios for the nature and evolution of the UCR.

[30] From its location seaward of the SDRs, the UCR could be an equivalent of the "rough basement" zone off SE Greenland described by *Hopper et al.* [2003]. The SDRs off SE Greenland terminate at a marked change in the morphology of the top of igneous crust, a rough, hummocky surface. Further seaward the rough basement morphology ends and there are again SDRs beneath a smooth basement surface, similar to the Argentine margin. *Hopper et al.* [2003], following *Planke et al.* [2000], interpreted the rough basement to mark a transition from subaerial to submarine eruptions.

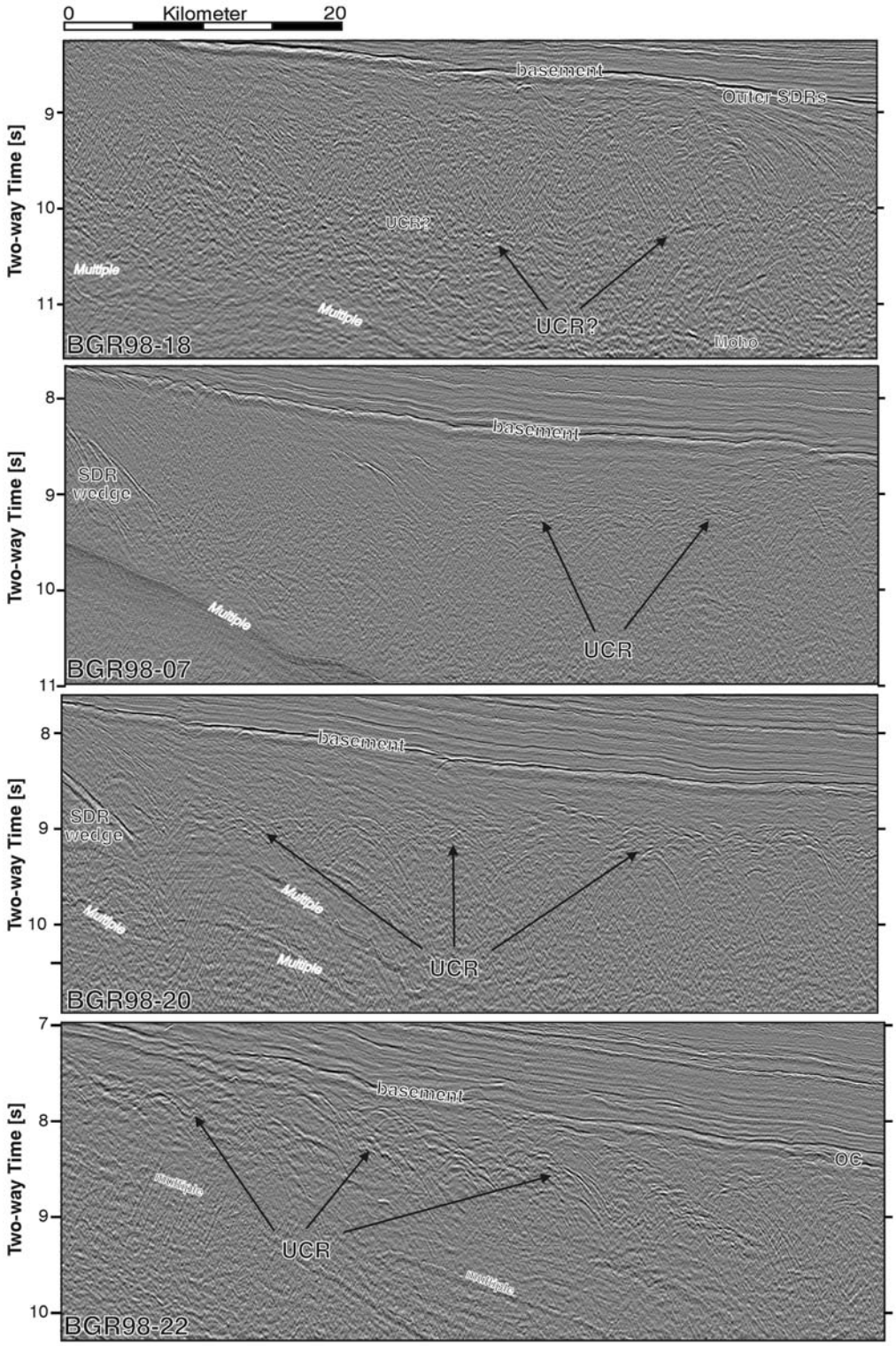

Figure 11. Enlarged seismic sections showing the highly diffractive, rough surface of the Upper Crustal Reflections (UCR) along strike, from south (fourth panel) to north (first panel) of the margin segment under study. Notations are as in Figure 4.

When the injection center is in a shallow marine environment (100–200 m water depth), eruptions tend to be explosive resulting in hyaloclastite flows [*Planke et al.*, 2000]. Occasionally, such shallow marine eruptions may build volcanoes reaching above sea level, resulting in subaerial volcanic flows. In seismic reflection data hyaloclastite flows appear as highly diffractive, rough surfaces [*Hopper et al.*, 2003]. We observe exactly the same reflection characteristics (Figure 11) and the UCR could therefore resemble the transition from subaerial to shallow submarine emplacement of flows. However, off the coast of SE Greenland the rough basement is in fact the acoustic basement; that is, it is not beneath a distinct smooth low-amplitude reflection. If we would follow this interpretation of submarine eruptions as the cause of the UCR, we have problems to explain what material fills the space between the UCR and the acoustic basement. Velocity modeling for this layer revealed velocities typical for volcanic/magmatic material [*Schnabel et al.*, 2008].

[31] Alternatively we may consider this zone as initial oceanic crust. In oceanic crust that formed at fast spreading ridges there are examples of upper crustal reflections at similar depth beneath a distinct top basement reflection [e.g., *Ranero et al.*, 1997; *Reston et al.*, 1999]. The origin of these reflections remains unclear. It could be the layer 2/3 boundary of oceanic crust (i.e., the base of the sheeted dikes), alteration at the base depth of hydrothermal circulation, an intracrustal low angle detachment, or a combination of any of these. Reflections at about 600–800 ms (TWT) beneath the top of the basement are probably too deep to represent the base of layer 2A [*Reston et al.*, 1999]. From the reflection characteristics of the UCR in our study area a detachment is unlikely since it will not form an irregular and hummocky surface. A possible explanation for the origin of the UCR could be that it marks the initiation of a magmatic-tectonic adjustment to a more uniform spreading ridge with the base of the sheeted dikes and the depth of hydrothermal circulation being possible candidates for the origin of the reflections.

[32] We do not yet have a final interpretation for the origin of the UCR. It may well be a combination of different sources, such as hydrothermal circulation and the layer 2/3 boundary and shallow marine eruptions. However, all the possibilities have one feature in common, namely submarine conditions during formation.

6.2. Formation of the SDRs

[33] Coming from the south, the first SDR wedge was extruded some 10 km north of the Colorado transfer zone. We follow the model initially proposed by *Hinz* [1981] and *Mutter et al.* [1982] and subsequently modified by, e.g., *Mutter* [1985], *Mutter and Karson* [1992], *Talwani et al.* [1995], and *Talwani and Abreu* [2000] and propose that the SDRs formed at a subaerially emergent spreading center by anomalously voluminous volcanism with long flow lengths (Figures 4 and 12). Before this took place, the lower crust west of the SDRs was likely heavily intruded, resulting in the high-velocity lower crustal body (Figure 12a).

[34] According to our interpretation, the SDRs furthest west and now furthest landward were emplaced first. Eventually one or several intrusions reached the surface and resulted in this volcanic flow unit (Figure 12b). During a period of magmatic stagnation erosion and weathering affected the top of this flow resulting in an unconformity. Continuing extension resulted in thinning of the crust but a stable magma chamber did not yet develop. Before the next volcanic pulse was initiated, the injection center migrated east and the second wedge was emplaced next to the first (Figure 12c). As before, this flow unit was exposed and eroded before the next flow was emplaced from an injection center located even farther east (Figure 12d). In the south, this second flow partly covers the first wedge, but the main part of this wedge is located seaward of the first SDR flows. Toward the north, the main SDR wedge 1 decreases in width and becomes increasingly buried beneath main SDR wedge 2 (Figure 6). SDR wedge 2, in contrast, shows a continuous or slightly increasing width and wedge 3 is irregularly distributed.

[35] Continuous stretching and subsidence eventually resulted in submergence of the proto–spreading center with the top of the feeder dykes now erupting under shallow water conditions. The UCR evolved and the depression that formed during further subsidence was presumably filled by volcanoclastics, ashes, tuffs and some minor volcanic flows (Figure 12e). Subsidence of the zone with flat-lying flows and the UCR continued as the rift propagated northward. The decreasing width of this zone toward the north can be explained by a combination of a triangle-shaped opening of the segment (see below) and increasing subsidence due to the stacked SDRs, resulting in a

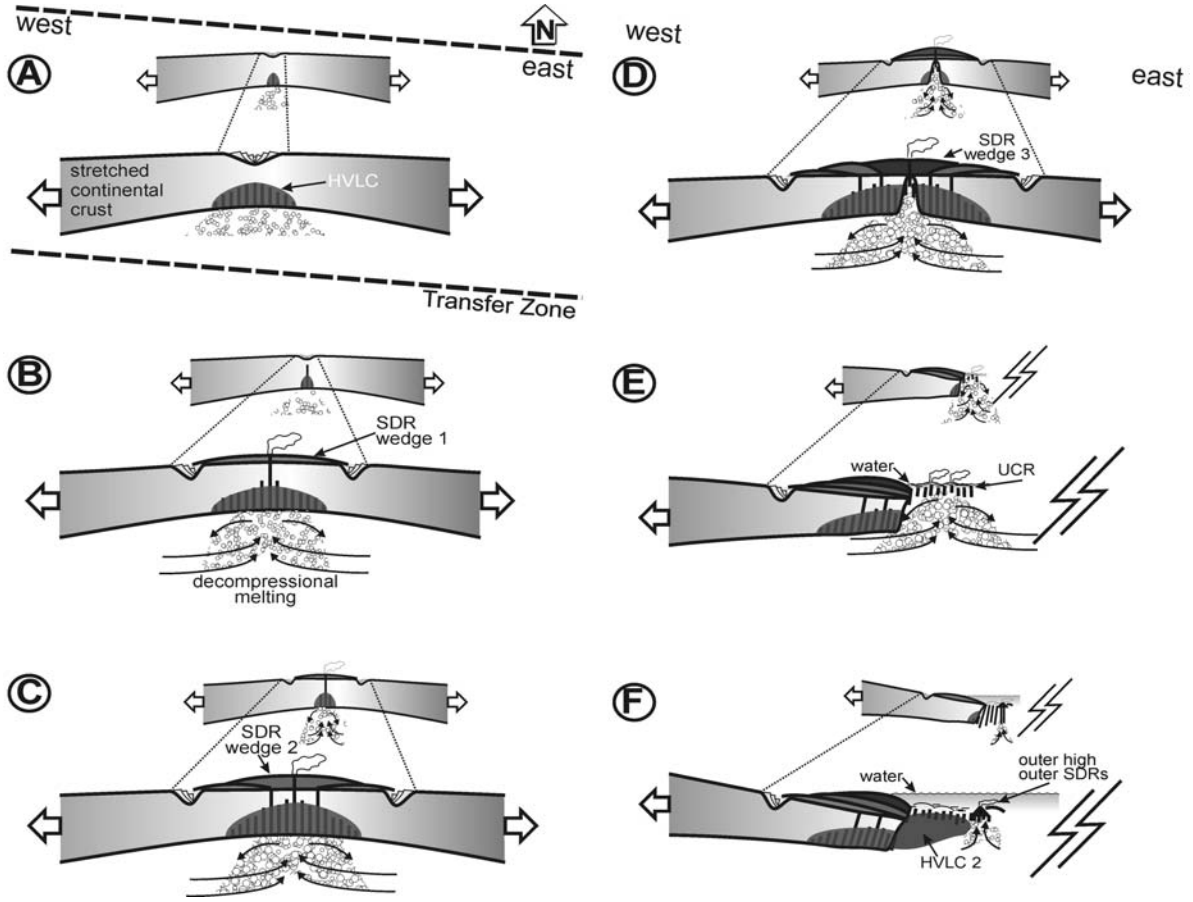

Figure 12. Sketch illustrating the evolution of the volcanic/magmatic features off Argentina in a margin segment bounded by transfer zones. A triangle-shaped opening of the margin segment is expected to result in different stretching along strike of the margin. There is some evidence for symmetric SDRs on both sides of the South Atlantic [*Bauer at al.*, 2000; *Gladczenko et al.*, 1997, 1998]; however, the eastern side in Figures 12a–12d is widely speculative. (a) Crustal thinning is attended by intrusions in the lower crust. HVLC is the landward high-velocity lower crustal body as derived from refraction seismic modeling [*Schnabel et al.*, 2008]. (b) Small-scale convection and active upwelling develops in the shallow mantle, and eventually, a feeder dyke breaks through the crust, and emplacement of the landward Inner SDRs occurs. (c) The injections center migrates seaward, and the next Inner SDR wedge is fed by a seaward located dyke. (d) This continues in combination with further extension and subsidence until all Inner SDRs are emplaced. (e) Seaward, the UCR develop supposedly as the top of feeder dykes under shallow marine conditions. (f) The next volcanic pulse results in the emplacement of the Outer High and Outer SDR wedge. These were likely emplaced under subaquateous condition. HVLC 2 is the seaward high-velocity lower crustal body as derived from refraction seismic modeling [*Schnabel et al.*, 2008].

shorter shallow water eruption phase in the north. In contrast long-lasting shallow water eruptions occur along the southern part of the margin segment.

[36] The Outer Highs/Outer SDRs are in our view related to a later phase of volcanism resulting in an emplacement of volcanic/magmatic material under subaqueous conditions (Figure 12f). This later pulse may correspond with the breakup of the next, northern margin segment. Additional subaqueous volcanic flows covering the UCR may be correlated with this phase. Eventually a stable magma chamber developed, resulting in the formation of mature oceanic crust seaward of the Outer SDRs.

6.3. Evolution of the Volcanic Rifted Margin

[37] At the northern edge of the magma-poor margin segment, at ~44°S, an irregular crustal reflection pattern similar in character to the UCR is present, which may be related to an evolving feeder dyke system (Figure 9). There may be an interbedding of volcanoclastics, tuff and ashes

between this reflection and the basement reflection, but no distinct SDRs developed. Across the Colorado transfer zone, a transition from magma-poor to magma-rich rifting takes place within about 10 km. Remarkably, the widest SDR wedges are found close to this transition, at the northern edge of the transfer zone. This abrupt change in emplaced magmatic volume leads us to consider alternative scenarios to the hypothesis that gradual along-margin variations in the thermal regime of the lithosphere and sublithospheric mantle (the traditional plume-driven model) are solely responsible for the transition from magma-poor to magma-rich volcanic margins. Gradual changes of mantel properties and dynamics would be expected to generate a smooth transition from magma-starved to volcanic rifting over at least a hundred or a few hundreds of kilometers.

[38] Additional findings that do not support this hypothesis (or its application to the Argentine margin), include the episodic emplacement of the SDRs and the proposed seaward migrating injection center for the SDRs during rifting. If the region were underlain by a stable, long-lasting thermal anomaly driving the extension, why would multiple phases of volcanism alternate with periods of magmatic stagnation? Such periods of stagnation are the best explanation for the presence of unconformities on top of the SDRs and the varying magnetic signals of the SDR wedges. Finally, northward decreasing volumes and production rates of melts as manifested by the SDR units (Table 1) are difficult to reconcile with the idea that the Tristan da Cunha plume caused the volcanic/magmatic edifices off Argentina. This plume hypothesis would predict a decrease of volcanism and magmatism with increasing distance from the plume head [*Franke et al.*, 2007].

[39] As pointed out by *Meyer et al.* [2007] there are unexplained aspects in the mantle plume concept and alternative models need to be developed. We suggest that the mode of opening of the South Atlantic substantially influenced the varying emplacement of the volcanic extrusives. Breakup by a successive northward unzipping of rift zones [e.g., *Jackson et al.*, 2000; *Nürnberg and Müller*, 1991] with a triangle-shaped opening of the about 400 km long margin segment as suggested by *Franke et al.* [2007] is expected to result in differential stretching along strike of the margin (Figure 12). This scissor-like opening explains that the injection center of the multiple SDR wedges migrated contemporaneously with ongoing extension in a seaward direction in the south, while it was more fixed in the northern part of this segment. In consequence, in the southern part of the margin segment the Inner SDRs were emplaced rather side by side, whereas in their northern part they were stacked on top of each other. Likewise the transitional zone between the Inner and Outer SDRs narrows in northern direction. In this scenario phases of volcanism correspond to high extension rates while phases of stagnation reflect small extension rates or temporary stagnation in the rifting process.

[40] The question remains whether this lithospheric-scale model is also capable of explaining the decreasing amounts of emplaced melts in northerly direction (Table 1). Modeling experiments of lithospheric extension differ in the predicted amount of melt that may be produced by small-scale convection and active upwelling in the shallow mantle. *Nielsen and Hopper* [2002] suggested that higher than average mantle temperatures are required to create the amount of melts observed on volcanic rifted margins, and small-scale convection is capable of producing small-scale melting anomalies only [*Nielsen and Hopper*, 2004]. However, *van Wijk et al.* [2001] suggested that a mantle plume is not always a prerequisite to generate a volcanic margin. A recent numerical modeling study proposed that small-scale convective instabilities during rifting are capable of explaining the origin of volcanic margins with moderate volumes of melts generated without the presence of a temperature anomaly in the sublithospheric mantle [*Simon et al.*, 2009]. The amount of melt being generated depends not only on the thermal structure of the lithosphere and sublithospheric mantle but also on the prerift lithosphere structure, rheology, and extension rates [*van Wijk et al.*, 2001, 2004; *Corti et al.*, 2003]. A well-defined time frame is crucial to the understanding of volcanism at any margin, but is not established for the Argentine margin yet. In addition, we do not deal with the crustal rheology and the thermal structure of the lithosphere and sublithospheric mantle, and focus on the SDRs only. Thus, we do not want to favor any particular model. However, our data provide structural constraints which these models should account for. Presuming that the transfer zones formed prominent lithospheric discontinuities at the onset of rifting, these are expected to have strongly influenced the generation of melts. An axial symmetrical small-scale mantle convection system may have developed all along the rifted margin segment [*van Wijk et al.*, 2004] with the

transfer zones having acted as rift propagation barriers (Figure 12). In this model decreasing extension rates toward the north along the margin segment under study result in decreasing volumes of melts. We do not exclude elevated mantle temperatures during rifting, however, we propose that a vast amount of the volcanic/magmatic structures found at this particular margin can be sufficiently explained if we consider that passive rifting processes controlled, at least partly, the production rates of melts.

7. Conclusions

[41] A dense grid of multichannel seismic data from the volcanic rifted margin off Argentina provides information on the architecture and distribution of large volume extrusive volcanic structures. This study presents a detailed analysis of a margin segment between 44°S and 41°S, i.e., between the Colorado and the Ventana transfer zones.

[42] Within this margin segment, there are two end-member styles of the emplaced volcanic/magmatic features:

[43] 1. In the south we found up to three major Inner SDRs, separated by unconformities; a wide area with a distinct, diffractive horizontal reflection band beneath the prominent low-frequency acoustic basement. Frequently an additional SDR wedge, occasionally bounded by an Outer High was identified. The dip of the Inner SDR wedges is not as steep as in the northern part of the study area.

[44] 2. In the north only one very thick, steeply dipping wedge is present. Internally, the SDR wedge is defined by a pattern of numerous, high-frequency divergent reflections. A narrow zone of diffractive horizontal reflections separates it from an additional Outer SDR wedge.

[45] Along-strike of the margin we observe a gradual transition from laterally juxtaposed Inner SDR wedges in the south to a vertically stacked wedge in the north. In the area of the multiple Inner SDRs, subsidence is considerably smaller than in the area of the single wedge. This and the absence of normal faults bounding the SDR wedges indicate that subsidence is controlled predominantly by loading.

[46] Subhorizontal Upper Crustal Reflections (UCR) are observed in between the Inner and the Outer SDR wedges, primarily in the southern area. It is a diffractive horizontal reflection band beneath the acoustic basement that deepens and becomes narrower toward the north. This reflection band may also be present at the transition from the sheared margin to the volcanic rifted margin segment, i.e., in a region where no SDRs developed. Outer Highs are widespread in the southern area of the margin segment but are sparse in the northern study area. Outer SDRs are common throughout the area.

[47] Based on the spatial separation, the unconformities and the varying magnetic signatures of the multiple Inner SDR wedges, we propose an episodic emplacement of the individual Inner SDRs. These volcanics likely were emplaced subaerially. It is proposed that the multiple Inner SDRs resulted from a seaward migrating injection center during rifting. The unconformities on top of the Inner SDRs are interpreted as the result of an erosion phase during magmatic stagnation. The UCR are tentatively interpreted as the result of being emplaced under shallow water conditions during formation. The Outer Highs/Outer SDRs may be related to a later phase of volcanism resulting in an emplacement under subaqueous conditions.

[48] Plume-driven models are the traditional explanation for the formation of volcanic rifted margins. However, the following observations along the studied margin segment are difficult to explain by this model: (1) The transition from magma-poor to magma-rich rifting takes place within only about 10 km. (2) The SDRs were emplaced episodically and the injection center for the multiple Inner SDRs likely migrated seaward during rifting. (3) The volumes of melts as manifested by the Inner SDR units decrease toward the Tristan da Cunha plume.

[49] A scissor-like opening of the margin segment under study explains both the migrating injection center of the multiple Inner SDR wedges in the south and the stacked SDRs in the north. We speculate that the varying amount of melts that were emplaced along strike of the margin segment are related to the mode of opening of the South Atlantic.

Acknowledgments

[50] We dedicate this manuscript to our research partner, our kind and valued friend Sönke Neben, who passed away suddenly and unforeseen in his forty-seventh year on 13 November 2009. Funding for this work was provided by the Federal Institute for Geosciences and Natural Resources (BGR). This is a contribution to project FR 2119/2-1 funded

by the Deutsche Forschungsgemeinschaft (German Research Foundation) within the priority program SAMPLE. We thank Hans Keppler and Joyce Miller for checking the language and grammar. Reviews from Sverre Planke and John Hopper and comments from the Associate Editor Romain Meyer and the Editor Vincent Salters helped improve the manuscript and are kindly acknowledged.

References

Austin, J. A., and E. Uchupi (1982), Continental-oceanic crustal transition of southwest Africa, *AAPG Bull.*, *66*(9), 1328–1347.

Bauer, K., S. Neben, B. Schreckenberger, R. Emmermann, K. Hinz, N. Fechner, K. Gohl, A. Schulze, R. B. Trumbull, and K. Weber (2000), Deep structure of the Namibia continental margin as derived from integrated geophysical studies, *J. Geophys. Res.*, *105*(B11), 25,829–25,853.

Blaich, O. A., et al. (2009), Crustal-scale architecture and segmentation of the Argentine margin and its conjugate off South Africa, *Geophys. J. Int.*, *178*, 85–105, doi:10.1111/j.1365-246X.2009.04171.x.

Clemson, J., et al. (1999), The Namib rift: A rift system of possible Karoo age, offshore Namibia, in *The Oil and Gas Habitats of the South Atlantic*, edited by N. R. Cameron et al., *Geol. Soc. Spec. Publ.*, *153*, 381–402.

Corti, G., J. Van Wijk, M. Bonini, D. Sokoutis, S. Cloetingh, F. Innocenti, and P. Manetti (2003), Transition from continental break-up to punctiform seafloor spreading: How fast, symmetric and magmatic, *Geophys. Res. Lett.*, *30*(12), 1604, doi:10.1029/2003GL017374.

Courtillot, V. (1982), Propagating rifts and continental breakup, *Tectonics*, *1*, 239–250, doi:10.1029/TC001i003p00239.

de Vera, J., et al. (2010), Structural evolution of the Orange Basin gravity-driven system, offshore Namibia, *Mar. Pet. Geol.*, *27*(1), 223–237, doi:10.1016/j.marpetgeo.2009.02.003.

Dunbar, J. A., and D. S. Sawyer (1989), Patterns of continental extension along the conjugate margins of the central and north Atlantic oceans and Labrador Sea, *Tectonics*, *8*, 1059–1077, doi:10.1029/TC008i005p01059.

Eagles, G. (2007), New angles on South Atlantic opening, *Geophys. J. Int.*, *168*(1), 353–361, doi:10.1111/j.1365-246X.2006.03206.x.

Ebinger, C., and N. Sleep (1998), Cenozoic magmatism in Africa: One plume goes a long way, *Nature*, *395*, 788–791, doi:10.1038/27417.

Eldholm, O., et al. (1989), Evolution of the Vøring Volcanic Margin, *Proc. Ocean Drill. Program Sci. Results*, *104*, 1033–1065.

Eldholm, O., et al. (1995), Volcanic margin concepts, in *Rifted Ocean-Continent Boundaries*, edited by E. Banda, M. Torné, and M. Talwani, pp. 1–16, Kluwer, Dordrecht, Netherlands.

Foulger, G. R., and J. H. Natland (2003), Is "hotspot" volcanism a consequence of Plate tectonics?, *Science*, *300*, 921–922, doi:10.1126/science.1083376.

Franke, D., et al. (2006), Crustal structure across the Colorado Basin, offshore Argentina, *Geophys. J. Int.*, *165*(3), 850–864, doi:10.1111/j.1365-246X.2006.02907.x.

Franke, D., et al. (2007), Margin segmentation and volcano-tectonic architecture along the volcanic margin off Argentina/Uruguay, South Atlantic, *Mar. Geol.*, *244*(1–4), 46–67, doi:10.1016/j.margeo.2007.06.009.

Gladczenko, T. P., et al. (1997), South Atlantic volcanic margins, *J. Geol. Soc.*, *154*, 465–470, doi:10.1144/gsjgs.154.3.0465.

Gladczenko, T. P., et al. (1998), Namibia volcanic margin, *Mar. Geophys. Res.*, *20*(4), 313–341, doi:10.1023/A:1004746101320.

Hinz, K. (1981), A hypothesis on terrestrial catastrophes: Wedges of very thick oceanward dipping layers beneath passive continental margins—Their origin and paleoenvironmental significance, *Geol. Jahrb., Reihe E*, *22*, 3–28.

Hinz, K., et al. (1999), The Argentine continental margin north of 48°S: Sedimentary successions, volcanic activity during breakup, *Mar. Pet. Geol.*, *16*(1), 1–25, doi:10.1016/S0264-8172(98)00060-9.

Hirsch, K. K., et al. (2009), Deep structure of the western South African passive margin—Results of a combined approach of seismic, gravity and isostatic investigations, *Tectonophysics*, *470*, 57–70, doi:10.1016/j.tecto.2008.04.028.

Hopper, J. R., T. Dahl-Jensen, W. S. Holbrook, H. C. Larsen, D. Lizarralde, J. Korenaga, G. M. Kent, and P. B. Kelemen (2003), Structure of the SE Greenland margin from seismic reflection and refraction data: Implications for nascent spreading center subsidence and asymmetric crustal accretion during North Atlantic opening, *J. Geophys. Res.*, *108*(B5), 2269, doi:10.1029/2002JB001996.

Jackson, M. P. A., et al. (2000), Role of subaerial volcanic rocks and mantle plumes in creation of South Atlantic margins: Implications for salt tectonics and source rocks, *Mar. Pet. Geol.*, *17*(4), 477–498, doi:10.1016/S0264-8172(00)00006-4.

Jacques, J. M. (2003a), A tectonostratigraphic synthesis of the Sub-Andean basins: Implications for the geotectonic segmentation of the Andean Belt, *J. Geol. Soc.*, *160*(5), 687–701, doi:10.1144/0016-764902-088.

Jacques, J. M. (2003b), A tectonostratigraphic synthesis of the Sub-Andean basins: Inferences on the position of South American intraplate accommodation zones and their control on South Atlantic opening, *J. Geol. Soc.*, *160*(5), 703–717, doi:10.1144/0016-764902-089.

King, S. D., and D. L. Anderson (1998), Edge-driven convection, *Earth Planet. Sci. Lett.*, *160*(3–4), 289–296, doi:10.1016/S0012-821X(98)00089-2.

Larsen, H. C., and A. D. Saunders (1998), Tectonism and volcanism at the southeast Greenland rifted margin: A record of plume impact and later continental rupture, *Proc. Ocean Drill. Program Sci. Results*, *152*, 503–534.

Leg 104 Shipboard Scientific Party (1986), Formation of the Norwegian Sea, *Nature*, *319*, 360–361, doi:10.1038/319360a0.

Martin, A. K. (1987), Plate reorganisations around southern Africa, hot-spots and extinctions, *Tectonophysics*, *142*(2–4), 309–316, doi:10.1016/0040-1951(87)90129-6.

Max, M. D., et al. (1999), Geology of the Argentine continental shelf and margin from aeromagnetic survey, *Mar. Pet. Geol.*, *16*(1), 41–64, doi:10.1016/S0264-8172(98)00063-4.

Menzies, M. A., et al. (2002), Characteristics of volcanic rifted margins, in *Volcanic Rifted Margins*, edited by M. A. Menzies et al., *Spec. Pap. Geol. Soc. Am.*, *362*, 1–14.

Meyer, R., J. van Wijk, and L. Gernigon (2007), The North Atlantic Igneous Province: A review of models for its formation, in *Plates, Plumes, and Planetary Processes*, edited by G. R. Foulger and D. M. Jurdy, *Spec. Pap. Geol. Soc. Am.*, *430*, 525–552.

Mutter, J. C. (1985), Seaward dipping reflectors and the continent-ocean boundary at passive continental margins, *Tectonophysics*, *114*(1–4), 117–131, doi:10.1016/0040-1951(85)90009-5.

Mutter, J. C., and J. A. Karson (1992), Structural processes at slow spreading ridges, *Science*, *257*, 627–634, doi:10.1126/science.257.5070.627.

Mutter, J. C., et al. (1982), Origin of seaward-dipping reflectors in oceanic crust off the Norwegian margin by "subaerial sea-floor spreading," *Geology*, *10*(7), 353–357, doi:10.1130/0091-7613(1982)10<353:OOSRIO>2.0.CO;2.

Nielsen, T. K., and J. R. Hopper (2002), Formation of volcanic rifted margins: Are temperature anomalies required?, *Geophys. Res. Lett.*, *29*(21), 2022, doi:10.1029/2002GL015681.

Nielsen, T. K., and J. R. Hopper (2004), From rift to drift: Mantle melting during continental breakup, *Geochem. Geophys. Geosyst.*, *5*, Q07003, doi:10.1029/2003GC000662.

Nürnberg, D., and R. D. Müller (1991), The tectonic evolution of the South Atlantic from Late Jurassic to present, *Tectonophysics*, *191*(1–2), 27–53, doi:10.1016/0040-1951(91)90231-G.

Planke, S., P. A. Symonds, E. Alvestad, and J. Skogseid (2000), Seismic volcanostratigraphy of large-volume basaltic extrusive complexes on rifted margins, *J. Geophys. Res.*, *105*(B8), 19,335–19,351.

Rabinowitz, P. D., and J. L. Labrecque (1979), The Mesozoic South Atlantic Ocean and evolution of its continental margins, *J. Geophys. Res.*, *84*(B11), 5973–6002, doi:10.1029/JB084iB11p05973.

Ranero, C. R., et al. (1997), Reflective oceanic crust formed at a fast-spreading center in the Pacific, *Geology*, *25*(6), 499–502, doi:10.1130/0091-7613(1997)025<0499:ROCFAA>2.3.CO;2.

Reston, T. J., C. R. Ranero, and I. Belykh (1999), The structure of Cretaceous oceanic crust of the NW Pacific: Constraints on processes at fast spreading centers, *J. Geophys. Res.*, *104*(B1), 629–644, doi:10.1029/98JB02640.

Roberts, D. G., et al. (1984a), Evolution of volcanic rifted margins: Synthesis of Leg 81 results on the west margin of Rockall Plateau, *Initial Rep. Deep Sea Drill. Proj.*, *81*, 883–911.

Roberts, D. G., et al. (1984b), Late Paleocene-Eocene volcanic events in the northern North Atlantic Ocean, *Initial Rep. Deep Sea Drill. Proj.*, *81*, 913–923.

Sandwell, D. T., and W. H. F. Smith (1997), Marine gravity from Geosat and ERS-1 altimetry, *J. Geophys. Res.*, *102*, 10,039–10,054, doi:10.1029/96JB03223.

Schnabel, M., et al. (2008), The structure of the lower crust at the Argentine continental margin, South Atlantic at 44°S, *Tectonophysics*, *454*(1–4), 14–22, doi:10.1016/j.tecto.2008.01.019.

Sibuet, J.-C., et al. (1984), Early evolution of the South Atlantic Ocean: Role of the rifting episode, *Initial Rep. Deep Sea Drill. Proj.*, *75*, 469–481.

Simon, K., et al. (2009), Dynamical modelling of lithospheric extension and small-scale convection: Implications for magmatism during the formation of volcanic rifted margins, *Geophys. J. Int.*, *176*, 327–350, doi:10.1111/j.1365-246X.2008.03891.x.

Skogseid, J. (2001), Volcanic margins: Geodynamic and exploration aspects, *Mar. Pet. Geol.*, *18*(4), 457–461, doi:10.1016/S0264-8172(00)00070-2.

Talwani, M., and V. Abreu (2000), Inferences regarding initiation of oceanic crust formation from the U.S. East Coast Margin and Conjugate South Atlantic Margins, in *Atlantic Rifts and Continental Margins*, *Geophys. Monogr. Ser.*, vol. 115, edited by W. Mohriak and M. Talwani, pp. 211–234, AGU, Washington, D. C.

Talwani, M., et al. (1995), The EDGE experiment and the U.S. Coast Magnetic anomaly, in *Rifted Ocean-Continent Boundaries: Proceedings of the NATO Advanced Research Workshop, Mallorca, Spain, 11–14 May 1994*, edited by E. Banda et al., pp. 155–181, Kluwer Acad., Dordrecht, Netherlands.

Uchupi, E. (1989), The tectonic style of the Atlantic mesozoic rift system, *J. Afr. Earth Sci.*, *8*(2–4), 143–164, doi:10.1016/S0899-5362(89)80021-1.

Unternehr, P., et al. (1988), South Atlantic fits and intraplate boundaries in Africa and South America, *Tectonophysics*, *155*(1–4), 169–179, doi:10.1016/0040-1951(88)90264-8.

van Wijk, J. W., and D. K. Blackman (2005), Dynamics of continental rift propagation: The end-member modes, *Earth Planet. Sci. Lett.*, *229*(3–4), 247–258, doi:10.1016/j.epsl.2004.10.039.

van Wijk, J. W., R. S. Huismans, M. ter Voorde, and S. A. P. L. Cloetingh (2001), Melt generation at volcanic continental margins: No need for a mantle plume?, *Geophys. Res. Lett.*, *28*(20), 3995–3998, doi:10.1029/2000GL012848.

van Wijk, J. W., et al. (2004), Crustal thickening in an extensional regime: Application to the mid-Norwegian Vøring margin, *Tectonophysics*, *387*(1–4), 217–228, doi:10.1016/j.tecto.2004.07.049.

White, R. S., and D. P. McKenzie (1989), Magmatism at rift zones: The generation of volcanic continental margins and flood basalts, *J. Geophys. Res.*, *94*, 7685–7729, doi:10.1029/JB094iB06p07685.

White, R. S., et al. (1987), Magmatism at rifted continental margins, *Nature*, *330*, 439–444, doi:10.1038/330439a0.